Available online at www.most.gov.bd

Volume 03, Issue (1), Page : 11-22, 2021

Ministry of Science and Technology
Government of The People's of Bangladesh
Bangladesh Secretariat, Dhaka.

Synthesis and DFT Studies of Glucopyranoside Dipentanoyl Esters

M. M. Matin

Bioorganic and Medicinal Chemistry Laboratory, Department of Chemistry, University of Chittagong, Chittagong, 4331, Bangladesh

Abstract

Sugar esters (SEs) with potential antimicrobial activity were found to be a better choice to solve the multidrug resistant (MDR) pathogens due to their less side-effect. In this respect, regioselective dimolar pentanoylation of methyl α-D-glucopyranoside using direct method furnished the 2,6-di-*O*-pentanoate indicating more reactivity of C-6 and C-2 hydroxyl groups. To develop glucopyranoside based potential antimicrobial agents, the dipentanoate product was further converted into four newer 3,4-di-*O*-acyl esters reasonably in good yields. Prediction of activity spectra for substances (PASS) indicated them as better antifungals than antibacterials as well as more potent anticarcinogenic agents than the antioxidant agents. These observations were rationalized by DFT based thermodynamic and docking studies with fungal CYP51 (4UYL) and SARS-CoV-2 main protease (6LU7).

Received: 14 January 2021
Revised: 30 June 2022
Accepted: 10 July 2022

DOI: https://doi.org/10.3329/JSciTR.v3i1.62803

Keywords: Regioselective acylation; 2,6-Di-*O*-pentanoyl-α-D-glucopyranoside; PASS predication; DFT calculation; Molecular docking; SARS-CoV-2 main protease

Introduction

Sugar esters (SEs), composed of hydrophilic carbohydrate and one or more lipophilic acyl groups, are involved in many diverse biological events in organisms from all kind of life (Dhavale and Matin, 2004; Guthrie and Honeyman, 1968; Matin *et al.,* 2001). They have great synthetic utility as versatile intermediates in the syntheses of many natural products due to the presence of multifunctional groups (Dhavale and Matin, 2005; Godoy *et al.,* 2016; Matin, 2008; Matin, 2016). In addition, SEs have broad spectrum applications in food, cosmetic and pharmaceutical industries (Neta *et al.,* 2015; Watanabe *et al.,* 2000; Matin *et al.,* 2015). For instance, glucopyranose, xylopyranose, mannose, fructose and galactose esters strongly inhibit growth of various organisms like *A. flavus*, *F. graminarium*, *M. separate*, *S. mutans* and *T. cinnabarinus* (Huang *et al.,* 2017; AlFindee *et al.,* 2018). Some of them have triple-negative-A breast cancer properties (Elmaidomy *et al.,* 2020) and SARS-CoV-2 main protease inhibition properties (Matin *et al.,* 2022).

*Corresponding author e-mail: mahbubchem@cu.ac.bd; mmmatin2004@yahoo.co.in

However, preparation of the desired SEs is facing multiple problems due to the presence of several secondary hydroxyl groups of similar reactivity (Petrova *et al.,* 2018; Kabir and Matin, 1994). Also, variable antimicrobial results are reported by different researchers (Petrova *et al.,* 2018; Kabir and Matin, 1994), and there are few reports on their molecular docking with different essential proteins (Ye and Hayes, 2017). Considering biological and synthetic importance of glucose molecule, several 2,6-di-*O*-pentanoyl esters were synthesized from methyl α-D-glucopyranoside (**1**), and DFT based thermodynamic and docking studies were conducted (Matin *et al.,* 2021a). The additional part of the series (**2**-**6**) are reported and discussed herein.

Materials and methods

All the reagents and solvents used were purchased from Merck (Germany) and were used as received, unless otherwise specified. Evaporations were carried out under reduced pressure at below 40 °C. Thin layer chromatography (TLC) was performed on Kieselgel GF_{254} and column chromatography (CC) was performed with silica gel G_{60}. FT-IR spectra were recorded on a FT-IR spectrophotometer (Shimadzu, IR Prestige-21) in $CHCl_3$ technique. ^{1}H NMR (400 MHz) spectra were recorded for solutions in $CDCl_3$ using tetramethylsilane (TMS) as an internal standard and *J* values are mentioned in Hz. For acylation, glucopyranoside **1** or its dipentanoyl ester **2** was dissolved in anhydrous pyridine and necessary acylating agent was added slowly (2.2 eq) to the solution at low temperature. Stirring was continued at room temperature for 10-12 h followed by quenching, extraction, drying and chromatographic purification which furnished pure ester product(s).

Syntheses

*Methyl 2,6-di-O-pentanoyl-α-D-glucopyranoside (**2**)*: Clear syrup; yield 48% [20]; R_f = 0.50 (with *n*-hexane/EA = 1/1); FT-IR ($CHCl_3$) υ_{max} (cm^{-1}): 3350-3460 (OH), 1755, 1740 (CO); ^{1}H NMR (400 MHz, $CDCl_3$): δ_H 4.88 (d, *J* = 3.6 Hz, 1H, H-1), 4.66 (dd, *J* = 10.0 and 3.7 Hz, 1H, H-2), 4.47 (dd, *J* = 12.1 and 5.0 Hz, 1H, H-6a), 4.25 (dd, *J* = 12.1 and 2.0 Hz, 1H, H-6b), 3.94 (t, *J* = 9.3 Hz, 1H, H-3), 3.73 (t, *J* = 9.7 Hz, 1H, H-4), 3.43 (ddd, *J* = 12.8, 9.9 and 2.9 Hz, 1H, H-5), 3.34 (s, 3H, OCH_3), 2.37 [t, *J* = 7.5 Hz, 4H, 2 × $CH_3(CH_2)_2CH_2CO$], 1.58-1.61 [m, 4H, 2 × $CH_3CH_2CH_2CH_2CO$], 1.33-1.37 [m, 4H, 2 × $CH_3CH_2(CH_2)_2CO$], 0.91 [t, *J* = 6.6 Hz, 6H, 2 × $CH_3(CH_2)_3CO$].

*Methyl 3,4-di-O-isopentanoyl-2,6-di-O-pentanoyl-α-D-glucopyranoside (**3**):* Oil; yield 94%; R_f = 0.53 (*n*-hexane/EA = 4/1); FT-IR ($CHCl_3$): 1756, 1750, 1748, 1738 cm^{-1} (CO); ^{1}H NMR (400 MHz, $CDCl_3$): δ_H 5.47 (t, *J* = 9.8 Hz, 1H, H-3), 5.04 (t, *J* = 9.8 Hz, 1H, H-4), 4.92 (d, *J* = 3.6 Hz, 1H, H-1), 4.88 (dd, *J* = 10.0 and 3.6 Hz, 1H, H-2), 4.24 (dd, *J* = 12.2 and 4.8 Hz, 1H, H-6a), 4.14 (dd, *J* = 12.2 and 2.2 Hz, 1H, H-6b), 3.95-3.99 (m, 1H, H-5), 3.38 (s, 3H, O-CH_3), 2.29-2.37 [m, 4H, 2 × $CH_3(CH_2)_2CH_2CO$], 2.08-2.22 (br m, 6H, 2 × $(CH_3)_2CHCH_2CO$], 1.55-1.61 [m, 4H, 2 × $CH_3CH_2CH_2CH_2CO$] 1.19-1.34 [m, 4H, 2 × $CH_3CH_2(CH_2)_2CO$], 0.86-0.93 [m, 18H, 2 × $(CH_3)_2CHCH_2CO$ and 2 × $CH_3(CH_2)_3CO$].

*Methyl 3,4-di-O-ocanoyl-2,6-di-O-pentanoyl-α-D-glucopyranoside (**4**)*: Thick syrup; yield 84%; R_f = 0.58 (*n*-hexane/EA = 4/1); FT-IR ($CHCl_3$): 1756, 1750, 1748, 1739 cm^{-1} (CO); ^{1}H NMR (400 MHz, $CDCl_3$): δ_H 5.51 (t, *J* = 10.0 Hz, 1H, H-3), 5.05 (t, *J* = 10.0 Hz, 1H, H-4), 4.95 (d, *J* = 3.8 Hz, 1H, H-1), 4.87 (dd, *J* = 10.0 and 3.8 Hz, 1H, H-2), 4.18 (dd, *J* = 12.2 and 4.8 Hz, 1H, H-6a), 4.12 (dd, *J* = 12.2 and 2.2 Hz, 1H, H-6b), 3.92-3.99 (m, 1H, H-5), 3.38 (s, 3H, O-CH_3), 2.18-2.34 [m, 8H, 2 × $CH_3(CH_2)_2CH_2CO$ and 2 ×

$CH_3(CH_2)_5CH_2CO$], 1.48-1.62 [m, 8H, 2 × $CH_3CH_2CH_2CH_2CO$ and 2 × $CH_3(CH_2)_4CH_2CH_2CO$], 1.18-1.39 [br m, 20H, 2 × $CH_3CH_2(CH_2)_2CO$ and 2 × $CH_3(CH_2)_4(CH_2)_2CO$], 0.86-0.93 [m, 12H, 2 × $CH_3(CH_2)_3CO$ and 2 × $CH_3(CH_2)_6CO$].

*Methyl 3,4-di-O-decanoyl-2,6-di-O-pentanoyl-α-D-glucopyranoside (**5**)*: Syrup; yield 86%; R_f = 0.61 (*n*-hexane/EA = 4/1); FT-IR ($CHCl_3$): 1759, 1748, 1733, 1730 cm^{-1} (CO); ^1H NMR (400 MHz, $CDCl_3$): δ_H 5.47 (t, *J* = 9.8 Hz, 1H, H-3), 5.04 (t, *J* = 9.8 Hz, 1H, H-4), 4.94 (d, *J* = 3.7 Hz, 1H, H-1), 4.88 (dd, *J* = 10.0 and 3.7 Hz, 1H, H-2), 4.18 (dd, *J* = 12.2 and 4.6 Hz, 1H, H-6a), 4.12 (dd, *J* = 12.2 and 2.2 Hz, 1H, H-6b), 3.93-3.97 (m, 1H, H-5), 3.37 (s, 3H, O-CH_3), 2.20-2.36 [m, 8H, 2 × $CH_3(CH_2)_2CH_2CO$ and 2 × $CH_3(CH_2)_7CH_2CO$], 1.49-1.63 [br m, 8H, 2 × $CH_3CH_2CH_2CH_2CO$ and 2 × $CH_3(CH_2)_6CH_2CH_2CO$], 1.18-1.38 [br m, 28H, 2 × $CH_3CH_2(CH_2)_2CO$ and 2 × $CH_3(CH_2)_6(CH_2)_2CO$], 0.88-0.92 [m, 12H, 2 × $CH_3(CH_2)_3CO$ and 2 × $CH_3(CH_2)_8CO$].

*Methyl 3,4-di-O-palmitoyl-2,6-di-O-pentanoyl-α-D-glucopyranoside (**6**)*: Semi-solid; yield 77%; R_f = 0.66 (*n*-hexane/EA = 4/1); FT-IR ($CHCl_3$): 1756, 1748, 1740, 1733 cm^{-1} (CO); ^1H NMR (400 MHz, $CDCl_3$): δ_H 5.48 (t, *J* = 9.8 Hz, 1H, H-3), 5.10 (t, *J* = 9.7 Hz, 1H, H-4), 4.92 (d, *J* = 3.6 Hz, 1H, H-1), 4.89 (dd, *J* = 10.0 and 3.6 Hz, 1H, H-2), 4.09-4.20 (m, 2H, H-6), 3.90-3.94 (m, 1H, H-5), 3.36 (s, 3H, O-CH_3), 2.22-2.38 [br m, 8H, 2 × $CH_3(CH_2)_2CH_2CO$ and 2 × $CH_3(CH_2)_{13}CH_2CO$], 2.06-2.10 (m, 4H, 2 × $CH_3CH_2CH_2CH_2CO$), 2.00-2.07 [m, 4H, 2 × $CH_3(CH_2)_{12}CH_2CH_2CO$], 1.62-1.71 (m, 8H, 2 × $CH_3(CH_2)_{10}(CH_2)_2(CH_2)_2CO$], 1.17-1.41 [br m, 44H, 2 × $CH_3CH_2(CH_2)_2CO$ and 2 × $CH_3(CH_2)_{10}(CH_2)_4CO$], 0.86-0.94 [m, 12H, 2 × $CH_3(CH_2)_3CO$ and 2 × $CH_3(CH_2)_{14}CO$].

PASS predication, DFT calculation and molecular docking (MD)

Web based PASS (Prediction of Activity Spectra for Substances; http://www.way2drug.com/passonline/) was used for the evaluation of antimicrobial activities of the compounds (Matin and Chakraborty, 2020). SMILES (simplified molecular-input line-entry system) of the optimized compounds were used to predict the PASS results and are designated as Pa (probability for active compound) and Pi (probability for inactive compound). Only activities with Pa>Pi are considered as possible for a particular compound in the scale 0 to 1.

$$\text{Gap} = [\varepsilon\text{LUMO} - \varepsilon\text{HOMO}] \quad (1)$$

$$\eta = \frac{\varepsilon LUMO - \varepsilon HOMO}{2} \quad (2)$$

$$S = \frac{1}{\eta} \quad (3)$$

Recently, DFT (density function theory) based quantum mechanical methods are widely used to predict thermal energies, molecular orbital (MO), and molecular electrostatic potential (MEP) properties (Matin *et al.,* 2020a). First of all, the basic geometry of methyl α-D-glucopyranoside (1) was taken from the online ChemSpider structure database. All the SEs 2-6 were drawn with the GaussView (5.0) program (Frisch et al., 2013). All these compounds were optimized at B3LYP/3-21G basis set using Gaussian 09 program. GaussSum 3.0 was used to get DOS plot. To visualize MEP online WebMO demo server was used. FMO,

HOMO, LUMO, HOMO-LUMO gap (equation 1), hardness (η, equation 2), and softness (S, equation 3) were determined from the optimized structures using the following equations:

Cytochrome P450 sterol 14α-demethylase is an important enzyme in ergosterol biosynthesis during fungal growth, and hence, molecular docking (MD) was conducted with sterol 14α-demethylase (4UYL, *Aspergillus fumigatus*). Also, considering present pandemic situation MD was conducted with SARS-CoV-2 main protease (M-pro; PDB ID: 6LU7). Standard procedure was used for protein and ligand preparation (Matin *et al.,* 2019a; Matin *et al.,* 2020b). For each ligand (compound), the best-docked pose with the highest negative docking score value was recorded.

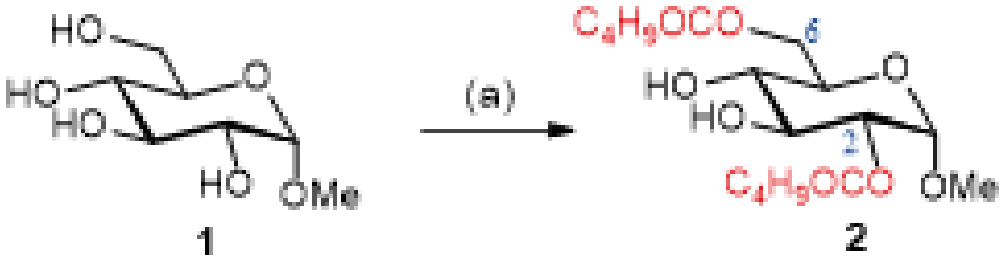

Scheme 1. Reagents & conditions: (a) Pyridine, C_4H_9COCl, 0 °C-rt, 12h, 48%

Results and discussion

*Synthesis of methyl 2,6-di-O-pentanoyl-α-D-glucopyranoside (**2**)*

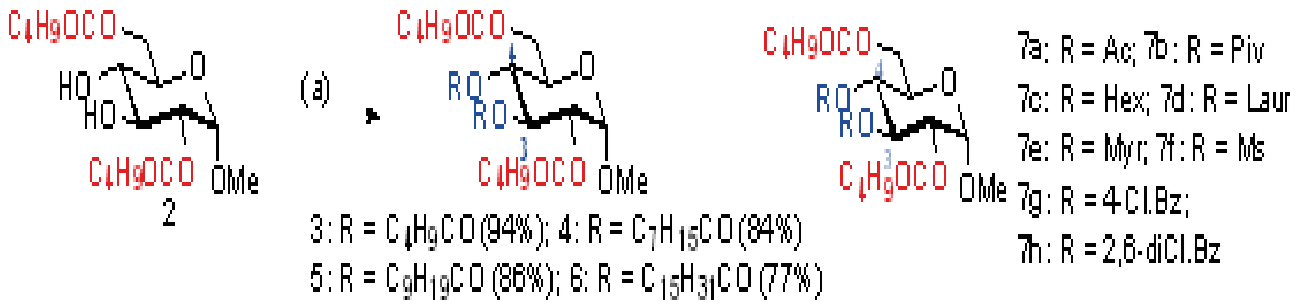

Scheme 2. (a) Pyridine, $(CH_3)_2CHCH_2COCl/C_7H_{15}COCl/C_9H_{19}COCl/ C_{15}H_{31}COCl$, 0 °C-rt, 10-12 h

Initially, dimolar pentanoylation of glucopyranoside *1* furnished the 2,6-di-*O*-pentanoate *2* as a syrupy mass in 48% (Scheme 1). The structure was confirmed by its FT-IR and ^{1}H NMR spectra and reported duly (Matin *et al.,* 2021a). The findings clearly indicated the more reactivity of 6-OH and 2-OH groups than 3-OH and 4-OH.

Synthesis of methyl 3,4-di-O-acyl-2,6-di-O-pentanoyl-α-D-glucopyranosides **3-6**

Having successful preparation of selective 2,6-di-*O*-pentanoate **2**, its 3,4-di-*O*-acyl esters **3-6** were prepared

Table 1. Predicted biological activities of 1-6 using PASS software

Drug	Biological Activity							
	Antibacterial		Antifungal		Anticarcinogenic		Antioxidant	
	Pa	Pi	Pa	Pi	Pa	Pi	Pa	Pi
1	0.541	0.013	0.628	0.016	0.731	0.008	0.667	0.004
2	0.568	0.011	0.695	0.010	0.723	0.008	0.481	0.007
3	0.566	0.011	0.689	0.010	0.555	0.015	0.408	0.011
4	0.551	0.012	0.673	0.011	0.614	0.012	0.463	0.008
5	0.551	0.012	0.673	0.011	0.614	0.012	0.463	0.008
6	0.551	0.012	0.673	0.011	0.614	0.012	0.463	0.008
TTC	0.694	0.005	0.523	0.023	-	-	-	-
FCZ	-	-	0.726	0.008	-	-	-	-

Pa = Probability 'to be active'; Pi = Probability 'to be inactive'; TTC = tetracycline; FCZ = fluconazole.

to get novel biologically potential glucopyranoside esters and some more related acylates 7a-h (Scheme 2) of the same project were already reported by Matin *et al.* (Matin *et al.,* 2021a). Initially, treatment of 2 with isopentanoyl chloride for 10 h followed by purification furnished an oil in excellent yield (94%, Scheme 2).

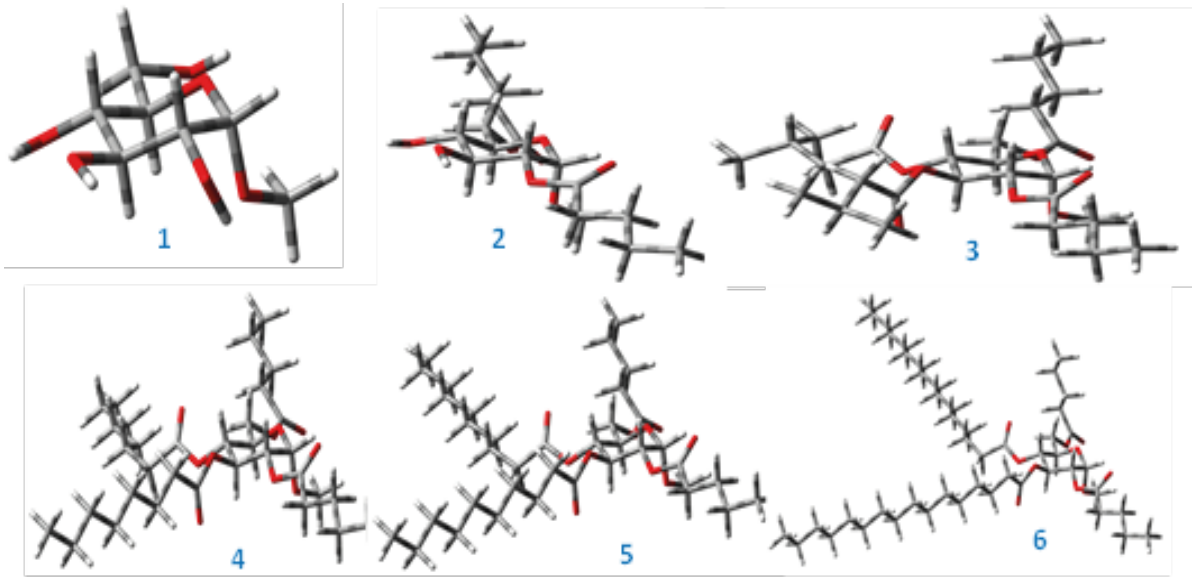

Fig. 1. DFT optimized (B3LYP/3-21G, 298.15 K, 1.0 atm) structures of 1-6 (tube model)

In its FT-IR spectrum, the presence of four carbonyl peaks and absence of hydroxyl bands clearly demonstrated the incorporation of two isovaleroyloxy groups in the molecule. This fact was further confirmed by the appearance of extra six protons in the aliphatic region (δ 2.08-2.22 as m) of its ^{1}H NMR spectrum. In addition, H-3 and H-4 shifted reasonable downfield at δ 5.47 and 5.04, respectively compared to its precursor molecule **2** (δ 3.94 and 3.73, respectively), and thus, confirmed the attachment of isopentanoyl groups at C-3 and C-4 positions of the molecule. Appearance of H-1 at δ 4.92 as doublet with small coupling constant (3.6 Hz) indicated its *cis*-relationship with H-2. As H-2 is axially oriented, hence, H-1 must be in equatorial i.e OMe group at C-1 is in axial (β) position. In corroboration of all these observation led to assign the structure of the compound as methyl 3,4-di-*O*-isopentanoyl-2,6-di-*O*-pentanoyl-α-D-glucopyranoside (**3**).

Similarly, separate treatment of dipentanoate **2** with dimolar amount of octanoyl chloride, decanoyl chloride and palmitoyl chloride followed by chromatographic purification gave corresponding ester **4, 5** and **6**, respectively in good yields (Scheme 2). All the compounds were well characterized by FT-IR and ^{1}H NMR spectral analyses.

Table 2. Molecular formula (MF), molecular weight (MW, g/mol), electronic energy (EE), enthalpy, Gibbs free energy (GFE) and dipole moment (DM) of 1-6.

Compound No.	MF	MW	EE (Hartree)	Enthalpy (Hartree)	GFE (Hartree)	DM (Debye)
1	$C_7H_{14}O_6$	194.18	-722.4733	-722.2348	-722.2887	2.6827
2	$C_{17}H_{30}O_8$	362.42	-1260.7287	-1260.2260	-1260.3198	4.0165
3	$C_{27}H_{46}O_{10}$	530.66	-1799.0007	-1798.2344	-1798.3643	4.2618
4	$C_{33}H_{58}O_{10}$	614.82	-2033.6045	-2032.6561	-2032.8086	4.4646
5	$C_{37}H_{66}O_{10}$	670.93	-2190.0099	-2188.9408	-2189.1070	4.3429
6	$C_{49}H_{90}O_{10}$	839.25	-2659.2261	-2657.7951	-2658.0016	4.4445

Computational biological activities: Prediction of activity spectra for substances (PASS)

PASS results, as shown in Table 1, indicated that the synthesized SEs had potential antimicrobial activities.

As indicated from Table 1, Pa for fungal pathogens (0.67<Pa<0.70) were higher than bacterial organisms (0.55<Pa<0.57) indicating that these SEs possess better antifungal potentiality. Also, they have better anticarcinogenic property (0.55<Pa<0.73) than the antioxidant property (0.40<Pa<0.48). Notably,

addition of fatty acyl groups like pentanoyl increased antifungal potentiality of glucopyranoside **1** which was higher than the tetracycline and comparable to standard antifungal fluconazole.

DFT optimized thermodynamic properties

To rationalize PASS predicted results of the SEs **2-6**, their thermochemical properties were calculated via optimizing their structures with the Gaussian 09 program (Frisch *et al.,* 2013). The density function theory

Table 3. Energy (eV) of HOMO, LUMO, energy gap, hardness, and softness of SEs 1-6

Drug	ε HOMO	ε LUMO	Gap	Hardness (η)	Softness (S)
1	-6.707	1.537	8.244	4.122	0.243
2	-6.927	0.004	6.931	3.466	0.289
3	-6.991	-0.223	6.768	3.384	0.296
4	-6.979	-0.210	6.769	3.385	0.295
5	-6.983	-0.218	6.765	3.383	0.296
6	-6.887	-0.210	6.677	3.339	0.299

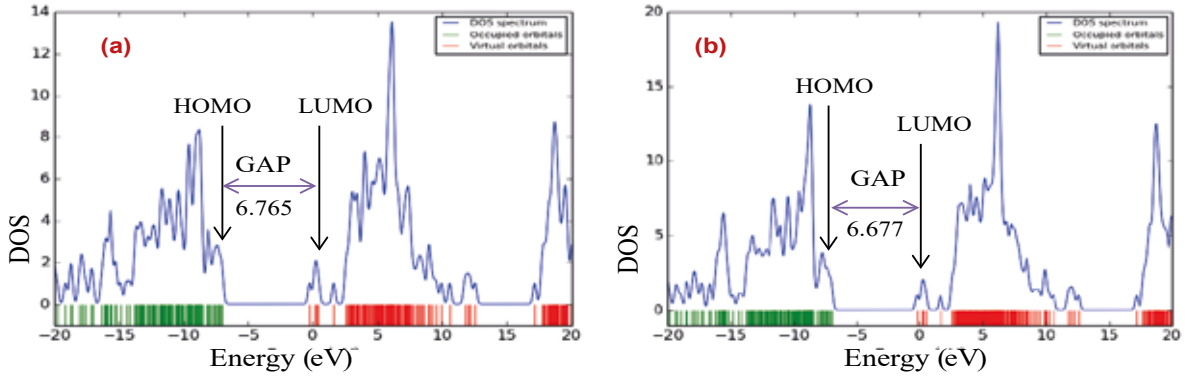

Fig. 2. HOMO-LUMO energy gap and DOS plot of (a) 5, and (b) 6.

(DFT, B3LYP/3-21G basis set) based optimized structure of glucopyranosides (at 298.15 K, 1.0 atm) are presented in Fig.1 which indicated that all the SEs had regular $^4C_1$ conformation with C1 symmetry.

Various thermodynamic properties of the optimized SEs **2-6** calculated at 298.15 K are presented in Table 2. With the addition of acyl groups and increase of chain length increased SEs RB3LYP energy (lower EE) indicating their more stability as compared to the glucopyranoside 1. For example, dipentanoate **2** has enthalpy -1260.2260 Hartee which upon addition of extra two palmitoyl groups (as in **6**) ΔH decreased to -2657.7951 Hartree. The lower enthalpy (ΔH) of the SEs further supported their greater stability. More precisely, the decreased EE and ΔH values are in consistent with the exothermic esterification reaction of carbohydrate molecules.

Again, Gibbs free energy (*G*) combines enthalpy and entropy into a single value and signifies spontaneity of a reaction when $G<0$. With increase of acyl chains hydrophobicity increases while *G* decreases. For example, *G* of dipentanoate **2** is -1260.7287 Hartree while tetra-*O*-acyl **3** is -1798.3643 Hartree and higher chain length containing palmitoate **6** is -2658.0016 Hartree. The huge relative lower *G* values (538 to

Table 4. Molecular docking score of 2-6 and some important antibiotics

Drugs	4UYL (kcal/mol)	6LU7 (kcal/mol)
1	-5.5	-5.2
2	-6.4	-5.1
3	-6.1	-4.9
4	-6.0	-4.7
5	-6.4	-5.3
6	-5.8	-4.8
Fluconazole	-6.5	-6.0
HCQ	-6.8	-4.6

Autodock vina was used for the calculation of docking score. For rigorous validation standard antibiotic fluconazole and HCQ were used. Generally, binding score <-6.0 kcal/mol is considered for good drug.

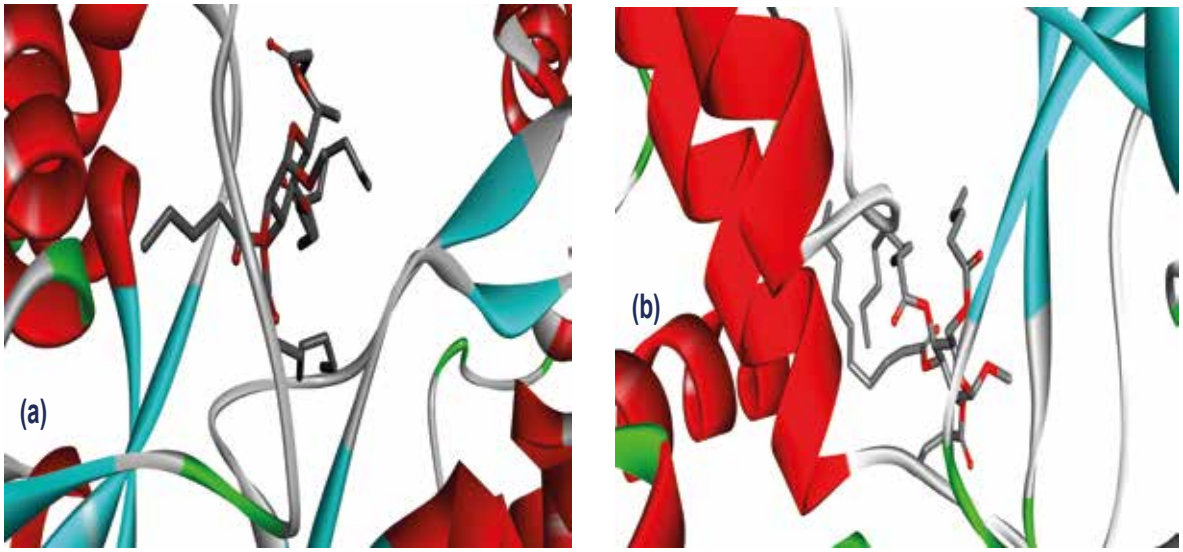

Fig. 3. 3D docking pose of complex- (a) compound 5-4UYL and (b) compound 5-6LU7.

1397.7 Hartree) indicated their spontaneous binding, and interaction with other substrates. Again, the SEs **2-6** had higher dipole moment (μ) than the non-ester **1** (Table 2) which indicated their net molecular polarity and binding affinity.

In the next step, frontier molecular orbitals (FMO) such as HOMO (highest occupied molecular orbital) and LUMO (lowest unoccupied molecular orbital) were calculated as these are involved in chemical reactivity (Ditchfield *et al.,* 1971). DFT (B3LYP/3-21G) optimized HOMO and LUMO energy levels of the glucopyranosides are presented in Table 3 (Fig. 2). It is clearly noted that with the addition of ester group(s) and increase of chain length gradually decreased HOMO-LUMO gap (6.6 to 6.9 eV) than the parent glucopyranoside **1** (8.224 eV). HOMO-LUMO gap ($\Delta\varepsilon$) of compound **5** (6.765 eV) and **6** (6.677 eV) are shown as DOS plot in Fig. 2. As the hardness is proportional to $\Delta\varepsilon$ (equation 2) the SEs hardness are decreased with the decreasing values of $\Delta\varepsilon$. Again, softness of the SEs **2-6** increased as this property is reciprocal to hardness (equation 3). The smaller molecular hardness and greater softness clearly demonstrated the bigger sizes, lower charge states and strong polarizable properties of the SEs **2-6** which are in complete accord with their higher dipole moment (> 4 Debye) than non-ester sugar **1** (2.6 Debye, Table 2).

Molecular docking (MD) results

As the glucopyranoside esters **2-6** showed better antifungal potentiality it was thought to justify by molecular docking (binding) with sterol 14α-demethylase (CYP51; PDB ID: 4UYL, Organism: *Aspergillus fumigatus*) and compared the results with standard antifungal drug fluconazole. It should be noted that most of the antifungal drugs are designed to inhibit CYP51 (Ahuja *et al.,* 2020; Matin *et al.,* 2019b). Again, some antifungal compounds were found to inhibit SARS-CoV-2 main proteases (Ahuja *et al.,* 2020; Matin *et al.,* 2019b). So, molecular docking was extended with COVID-19 main protease (PDB ID: 6LU7) and compared with the hydroxychloroquine (HCQ). The binding energies of all the SEs **2-6** are shown in Table 4.

It was clear from Table 4 that the glucopyranoside esters **2-6** had better docking (binding) energy (-5.8 to -6.4 kcal/mol) with antifungal related 4UYL than SARS-CoV-2 main protease 6LU7 (-4.7 to -5.3 kcal/mol) (Fig. 3). However, the binding energy of **2-6** was higher than that of the hydroxychloroquine (-4.6 kcal/mol). Thus, the synthesized esters **2-6** could be used as promising antifungal agents compared to COVID-19 main protease inhibitors.

Conclusion

Methyl α-D-glucopyranoside (**1**) upon dimolar pentanoylation showed selectivity at C-2 and C-6 positions. The dipentanoate **2**, thus obtained, was further converted to four novel 3,4-di-*O*-acylates **3-6** with four fatty acyl chains (5C-16C). PASS predication indicated that these SEs possess better antifungal and anticarcinogenic potentiality. Thermodynamic and molecular orbital calculations showed that these SEs are more stable. Molecular binding (docking) indicated that that **2-4** had better antifungal potentiality than that of COVID-19 main protease inhibition.

Acknowledgments

This research work was supported by the Ministry of Science and Technology, Bangladesh (Sl. no. 551, Physical Science, 2019-2020).

References

Ahuja R, Sidhu A, Bala A, Arora D and Sharma P 2020. Structure based approach for twin-enzyme targeted benzimidazolyl-1,2,4-triazole molecular hybrids as antifungal agents. *Arabian J. Chem.* **13:** 5832-5848.

AlFindee MN, Zhang Q , Subedi YP, Shrestha JP, Kawasaki Y, Grilley M, Taemoto JY and Chang CWT 2018. One-step synthesis of carbohydrate esters as antibacterial and antifungal agents. *Bioorg. Med. Chem.* **6**(3): 765-774.

Damme EV, Meyer SD, Bojkova D, Ciesek S, Cinatl J, Jonghe SD, Jochmans D, Leyssen P, Buyck C, Neyts J and Loock J 2020. In vitro activity of Itraconazole against SARS-CoV-2. bioRxiv.

Dhavale DD and Matin MM 2004. Selective sulfonylation of 4-C-hyroxymethyl-β-L-threo-pento-1, 4-furanose: Synthesis of bicyclic diazasugars. Tetrahedron **60**(19): 4275-4281. https://doi.org/10.1016/j.tet.2004.03.034

Dhavale DD and Matin MM 2005. Piperidine homoazasugars: Natural occurrence, synthetic aspects and biological activity study. *Arkivoc* **3:** 110-132.

Ditchfield R, Hehre WJ and Pople JA 1971. Self-Consistent Molecular-Orbital Methods. IX. An Extended Gaussian-Type Basis for Molecular-Orbital Studies of Organic Molecules. J. Chem. Physics **54:** 724.

Elmaidomy AH, Mohammed R and Owis AI 2020. Triple-negative breast cancer suppressive activities, antioxidants and pharmacophore model of new acylated rhamnopyranoses from Premna odorata. RSC Adv. **10:** 10584-10598.

Frisch MJ, Trucks GW, Schlegel HB, Scuseria GE, Robb MA, Cheeseman JR, Scalmani G, Barone V, Petersson GA and and Nakatsuji H 2013. Gaussian 09, Gaussian Inc. Wallingford CT.

Godoy LC, Arrizon J, Baez DA, Plou FJ and Sandoval G 2016. Synthesis and emulsifying properties of carbohydrate fatty acid esters produced from Agave tequilana fructans by enzymatic acylation. *Food Chem.* **204:** 437-443.

Guthrie RD and Honeyman J 1968. An Introduction to the Chemistry of Carbohydrates, 3rd Ed, Oxford (UK).

Huang X, Zhang B and Xu H 2017. Synthesis of some monosaccharide-related ester derivatives as insecticidal and acaricidal agents. Bioorg. Med. Chem. Lett. **27:** 4336-4340.

Kabir AKMS and Matin MM 1994. Regioselective acylation of a derivative of L-rhamonse using the dibutyltin oxide method. *J. Bangladesh Chem. Soc.* **7**(1): 73-79.

Kabir AKMS and Matin MM 1996. Selective pivaloylation of some D-glucose derivatives. Chittagong Univ. Studies, *Part II: Sci.* **20**(2): 105-111.

Kabir AKMS, Matin MM, Bhuiyan MMR and Rahim MA 2001. Synthesis and characterization of some acylated derivatives of D-mannose. *Chittagong Univ. J. Sci.* **25**(1): 65-73.

Kabir AKMS, Rahman MS, Matin MM, Bhuiyan M MR and Ali M 2001. Antimicrobial activities of some D-glucose derivatives. *Chittagong Univ. J. Sci.* **25**(1): 123-128.

Matin MM 2008. Synthesis of D-glucose derived oxetane: 1,2-O-Isopropylidene-4-(S)-3-O,4-C-methylene-5-O-methanesulfonyl-β-L-threo-pento-1,4-furanose. *J. Appl. Sci. Res.* **4**(11): 1478-1482.

Matin MM, Bhuiyan MMH, Hossain MM and Roshid MHO 2015. Synthesis and comparative antibacterial studies of some benzylidene monosaccharide benzoates. *J. Turk. Chem. Soc. Sect. A: Chem.* **2**(4): 12-21.

Matin MM 2016. Synthesis and Glycosidase Inhibitory Activity of Azasugars, Lambert Academic Publishing (Germany), pp 1-233.

Matin MM, Bhattacharjee SC, Chakraborty P and Alam MS 2019a. Synthesis, PASS predication, in vitro antimicrobial evaluation and pharmacokinetic study of novel n-octyl glucopyranoside esters. Carbohydr. Res. **485:** 107-812.

Matin MM, Bhuiyan MMH, Kabir E, Sanaullah AFM, Rahman MA, Hossain ME and M Uzzaman 2019b. Synthesis, characterization, ADMET, PASS predication, and antimicrobial study of 6-O-lauroyl mannopyranosides. *J. Mol. Struct.* **1195:** 189-197.

Matin MM and Chakraborty P 2020. Synthesis, spectral and DFT characterization, PASS predication, antimicrobial, and ADMET studies of some novel mannopyranoside esters. *J. Appl. Sci. Process Eng.* **7**(2): 572-586.

Matin MM, Hasan MS, Uzzaman M, Bhuiyan MM H., Kibria SM, Hossain ME and Roshid MHO 2020a. Synthesis, spectroscopic characterization, molecular docking, and ADMET studies of mannopyranoside esters as antimicrobial agents. *J. Mol. Struct.* **1222:** 128-821.

Matin MM, Chakraborty P, Alam MS, Islam MM and Hanee U 2020b. Novel mannopyranoside esters as sterol 14α-demethylase inhibitors: Synthesis, PASS predication, molecular docking, and pharmacokinetic studies. *Carbohydr. Res.* **496:** 108-130.

Matin MM, Chowdhury SA, Bhuiyan MMH, Kawsar SMA and Alam MA 2021a. Glucopyranoside dipentanoyl esters: Synthesis, PASS predication, antimicrobial and in silico ADMET studies. *J. Sci. Res.* **13**(1): 221-235.

Matin MM, Islam N, Siddika A and Bhattacharjee SC 2021b. Regioselective synthesis of some rhamnopyranoside esters for PASS predication, and ADMET studies. *J. Turk. Chem. Soc. Sect. A: Chem.* **8**(1): 363-374.

Matin MM, Uzzaman M, Chowdhury SA and Bhuiyan MMH 2022. *In vitro* antimicrobial, physicochemical, pharmacokinetics, and molecular docking studies of benzoyl uridine esters against SARS-CoV-2 main protease. *J. Biomol. Struct. Dyn.* **40**(8): 3668-3680.

Neta NS, Teixeira JA and Rodrigues LR 2015. Sugar ester surfactants: enzymatic synthesis and applications in food industry. *Crit. Rev. Food Sci. Nutr.* **55:** 595-610.

Petrova KT, Barros MT and Calhelha RC 2018. Antimicrobial and cytotoxic activities of short carbon chain unsaturated sucrose esters. *Med. Chem. Res.* **27:** 980-988.

Watanabe T, Katayama S, Matsubara M, Honda Y and Kuwahara M 2000. Antibacterial carbohydrate monoesters suppressing cell growth of Streptococcus mutans in the presence of sucrose. *Curr. Microbiol.* **41:** 210-213.

Ye R and Hayes DG 2017. ***In:*** Frontiers in Bioactive Compounds (Bentham Science) **2:** 124-145.